A Switched Electrical Model with Thermal Effects for Li-ion Batteries

S. Baccari, *Senior Member IEEE*, S. Sagnelli, F. Vasca, *Senior Member IEEE*, L. Iannelli, *Senior Member IEEE*

***Abstract*— A dynamic model for Li-ion batteries based on an equivalent switched electrical circuit is proposed. The switching topology of the model allows one to discriminate the model parameters for charging, discharging and relaxation phases. Thermal effects and the reversible entropic heat are taken into account, too. The proposed model is shown to require a lower number of parameters to be identified with respect to the classical equivalent circuit battery model. An identification procedure for determining the electrical and thermal model parameters is defined and its effectiveness is verified through experimental results.**

I. Introduction

Battery packs are used in several applications, ranging from cellphones to spacecrafts and automobiles. A battery pack is composed of a suitable number of individual cells arranged in either series or parallel configuration in order to store energy and provide the necessary electrical power to the devices. The need for increasing energy, power density and life cycle has spurred development towards more efficient batteries and battery management systems that monitor the electrical and thermal cell variables [1], [2]. In order to guarantee a good battery health and to prevent failures, individual battery cells are rigorously tested: the maximum charge capacity, peak voltage, internal resistance, discharge rate, total battery current are the main parameters to be characterized and monitored. In particular, for the analysis of thermal effects and distribution, several temperature sensors are suitably located on the battery surface. Moreover, the management of the charge/discharge cycle plays a crucial role in order to guarantee the battery health during its lifetime.

The strict constraints and required performance together with the variety of operative scenarios, justify the need for using battery models since the design phase of its management system [3]. Indeed, during the real use of a battery, dedicated measurement procedures for the evaluation of the battery state are not easy to be implemented. For example, the battery integrated in a satellite for low earth orbit missions has to be used continuously without any rest or open circuit operations [4], [5]. Equivalent circuit models for simulating the operating behavior of Li-ion batteries have been widely used in the automotive and the renewable energy fields by showing a good trade-off between the accuracy and model complexity [6], [7]. On the other hand, one of the major issues for a good battery lumped parameters model is still the determination of its parameters [8]. The characterization of Li-ion batteries through the estimation of their parameters is a topic which received a remarkable attention in the literature over the last decade. A high accuracy battery model has to take account of the equivalent electrical parameters as function of the state of charge and the temperature. The state of charge estimation is critical for the battery energy management and protection [9]. It plays a fundamental role in assessing remaining battery lifetime, protection against overcharging and accidental over-discharging, fault detection and for a safe and reliable operation of the battery [10]. Although there are some approaches available [11], the design of suitable off-line testing setup and procedures dedicated to the specific battery application is still a challenging task. In particular, one of the phenomena which must be considered is the so called battery relaxation [12]: after the end of a charging or discharging sequence, the battery voltage keeps evolving towards a finite value, during hours or even days, although no current is exchanged with the battery, and the cell goes to a steady state condition by changing the output voltage.

The battery model proposed in this paper is aimed to represent the electrical and thermal behaviors during charging, discharging and relaxation phases. A procedure for the identification of the model parameters starting from battery datasheet information is described. The battery model parameters identification is based on a multi-parameters optimization process that minimizes the error between the modelled process output and the experimental data over the full charging and discharging process. The identification consists of two phases, at first the electrical model with constant thermal dependencies is used and then the thermal part is identified.

The rest of the paper is organized as follows. In Sec. II the switched electrical battery model is described. Section III deals with the identification process for the model parameters and the hardware architecture implemented for the experimental battery characterization. The experimental results are discussed in Sec. IV. Conclusions are summarized in Sec. V.

II. Switched battery model

In this section the proposed switched model of the battery is presented. The model takes origin from the typical representation of the battery in terms of an equivalent electrical circuit with three resistor-capacitor branches which is able to capture the battery relaxation phases too. The proposed model can be presented by considering two different interlaced subsystems: a switched electrical subsystem and a

The authors are with Department of Engineering, University of Sannio, Benevento, Italy, *silvio.baccari@unisannio.it*, *ssagnelli@unisannio.it*, *vasca@unisannio.it*, *luiannel@unisannio.it*.

thermal subsystem.

A. Equivalent electrical circuit with relaxation

A typical representation of a battery in terms of an equivalent electrical circuit is shown in Fig. 1, see [13]. The electrical subsystem considers as input the current i, as state variables the internal battery voltages v_1, v_2 and v_3 and the state of charge Soc, as output variable the battery voltage v. The current is assumed with positive sign when the cell acts as an instantaneous electrical power generator and negative during the battery charging operating conditions.

The variable OCV represents the open circuit voltage. A series resistance R_0 considers the ohmic voltage drop due to the resistance of the electrolyte, the pins and the active material. The parallel of R_1 and C_1 is used to represent the slow dynamics of the model while the other two RC branches capture the fast electrical dynamics. The dependencies of the parameters R_0, R_2, C_2 and the voltage OCV on the state of charge Soc and the temperature T will be discussed later on.

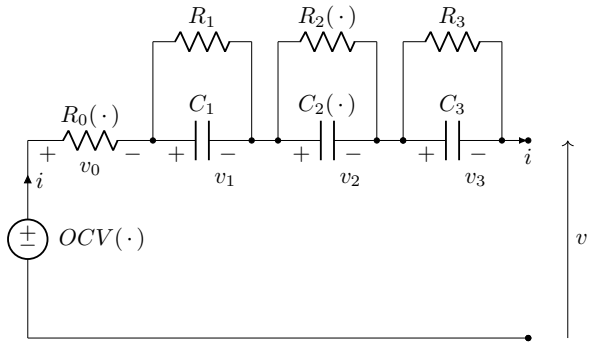

Fig. 1. Equivalent circuit model (3RC).

The Soc is obtained by integrating the following differential equation

$$Q\frac{\mathrm{d}}{\mathrm{d}t}Soc = -i, \tag{1}$$

where $Soc \in [0,1]$, Q is the battery capacity and the coulombic battery efficiency is equal to one. In general, Q depends on the current i (discharge rate effect) and on the battery internal temperature T, see [14] and [15], respectively. For the levels of temperatures and currents considered in our analysis we can assume constant value for the battery capacity.

By applying the Kirchhoff current law to the circuit in Fig. 1, the three internal voltage dynamic equations can be written as

$$C_k\frac{\mathrm{d}}{\mathrm{d}t}v_k = -\frac{1}{R_k}v_k + i \tag{2}$$

with $k = 1, 2, 3$.

The battery voltage v is the output of the model and, by considering the circuit in Fig. 1 can be written as

$$v = OCV - R_0 i - v_1 - v_2 - v_3 \tag{3}$$

where OCV is the open circuit voltage and R_0 is the internal resistance.

B. Switched equivalent circuit

The proposed switched equivalent circuit of the battery model is represented in Fig. 2. The dynamic equations of the model are the Soc state equation (1) together with the electrical equations which can be obtained by applying the Kirchhoff laws to the circuit in Fig. 2, thus obtaining

$$C_s\frac{\mathrm{d}}{\mathrm{d}t}v_1 = -\frac{1}{R_s + R_0}v_1 + \frac{R_0}{R_s + R_0}i \tag{4a}$$

$$C_2\frac{\mathrm{d}}{\mathrm{d}t}v_2 = -\frac{1}{R_2\delta + \hat{R}_2(1-\delta)}v_2 + i \tag{4b}$$

where the switching variable $\delta \in \{0, 1\}$ is equal to 1 when the battery current is different from zero and it is zero otherwise, i.e. during the relaxation phase.

The series connection of R_s and C_s plays the role of a sort of snubber. By considering (4) at steady state it is $v_1 = R_0 i$ which means that a suitable choice of C_s allows one to make negligible the influence of R_s and C_s after a short time interval of the charging and discharging phases at constant currents. Instead, when there is a step change of the current to zero, the relaxation phase is characterized by the exponential decays to zero of v_1 and v_2.

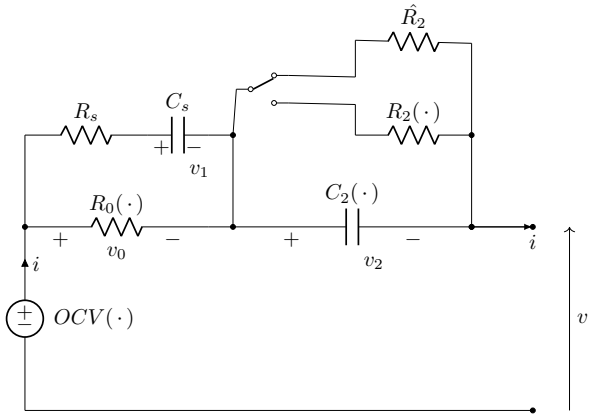

Fig. 2. Equivalent switched circuit of the proposed electrical subsystem model.

The battery voltage v is the output of the electrical subsystem model and can be obtained by applying the Kirchhoff voltage law to the circuit in Fig. 2 which allows one to write

$$v = OCV - \frac{R_0}{R_s + R_0}v_1 - v_2 - \frac{R_0 R_s}{R_s + R_0}i. \tag{5}$$

The expression (5) highlights that the presence of a nonzero R_s, combined with R_0, contributes to the well-known discontinuity of the battery voltage v in the presence of a step change of the current. For the classical equivalent circuit in Fig. 1, an analogous discontinuous behavior of v is only due to R_0, see (3).

C. Dependencies on state of charge and temperature

The parameters R_0, R_2, C_2 and the voltage OCV in Fig. 1 and Fig. 2 depends on Soc and T.

A typical dependence of R_0 on the state of charge and temperature can be defined through the following expression

$$R_0(T, Soc) = b_0 + b_1 Soc + b_2 \Delta_T + b_4(1 - e^{b_3 Soc}), \quad (6)$$

with Δ_T being a normalized temperature given by

$$\Delta_T = \frac{T - T_a}{T_a}, \quad (7)$$

T_a is the ambient temperature and $\{b_j\}_{j=0}^4 = \{b_0, \ldots, b_4\}$ are parameters to be identified, see [16] for details.

The resistor R_2 and the capacitor C_2 depends on the state of charge. In particular, a typical assumption is to consider R_2 to depend bilinearly on the current and Soc and exponentially on the temperature, while for C_2 a second order dependence on Soc can be considered, see [16]. Then the capacitor and the resistor dependencies can be expressed as

$$R_2(Soc, i, T) = d_0 + d_1 i Soc + d_2 \Delta_T + d_3 \Delta_T^2 \quad (8a)$$

$$C_2(Soc) = f_0 + f_1 Soc + f_2 Soc^2 \quad (8b)$$

where $\{d_j\}_{j=0}^3 = \{d_0, \ldots, d_3\}$ and $\{f_j\}_{j=0}^2 = \{f_0, \ldots, f_2\}$ are the sets of parameters to be identified.

The relation between OCV and Soc also depends on the battery current and temperature [17]. The following nonlinear function for the open circuit voltage has been considered

$$\begin{aligned} OCV(Soc, T) =& a_0 + a_1(1 - e^{a_2 Soc}) + a_3 \Delta_T + a_4 \Delta_T^2 \\ &+ a_5 Soc + a_6 Soc^2 + a_7 Soc^3 \\ &+ a_8 Soc \Delta_T \end{aligned} \quad (9)$$

with $\{a_j\}_{j=0}^8 = \{a_0, \ldots, a_8\}$ parameters to be identified, see [18] for details.

D. Thermal subsystem model

In order to take into account the thermal effects on the battery electrical behavior, the battery temperature T is considered as a further state variable.

The thermal model allows the computation of the cell temperature time evolution by considering as inputs the ambient temperature T_a and the power P_{diss} dissipated in the battery for the Joule effect and other inefficiencies [19]. The thermal dynamic equation can be written as

$$C_{th} \frac{\mathrm{d}}{\mathrm{d}t} T = -\frac{1}{R_{th}}(T - T_a) + P_{diss} - iT \frac{\partial OCV}{\partial T} \quad (10)$$

where R_{th} and C_{th} are the equivalent thermal resistance and capacity, respectively. The term on the right hand side of (10) with the partial derivative of OCV with respect to the temperature represents the reversible entropic heat. This term is responsible of the possible battery temperature decrease when a constant current step determines the start of a charging phase [20].

The power P_{diss} is obtained by neglecting the contributions of the resistors different from R_0 and the variation of R_0 for high values of Soc. Therefore, from (6) one can write

$$P_{diss}(T, i) = R_0(T, 1) i^2 = R_0(T_a, 1) i^2 + b_2 \Delta_T i^2 \quad (11)$$

with

$$R_0(T_a, 1) = b_0 + b_1 + b_4(1 - e^{b_3}) \quad (12)$$

obtained from (6). By substituting (9) and (11) in (10) one obtains

$$\begin{aligned} C_{th} \frac{\mathrm{d}}{\mathrm{d}t} T =& -\frac{1}{R_{th}}(T - T_a) + R_0(T_a, 1) i^2 + b_2 \Delta_T i^2 \\ &- i \frac{T}{T_a} \left(a_3 + 2 a_4 \Delta_T + a_8 Soc\right). \end{aligned} \quad (13)$$

The complete model of the battery consists of the dynamic electrical equations (1) and (4) together with the thermal dynamic equation (13). The fourth order system with state variables Soc, v_1, v_2 and T is highly nonlinear because of the dependencies $R_0(T, Soc)$ given by (6), $R_2(Soc, i, T)$ given by (8a), $C_2(Soc)$ given by (8b) and $OCV(Soc, T)$ given by (9). The parameters of the model are: Q, R_s, C_s, $\hat{R}_2$, C_{th}, R_{th}, $\{a_j\}_{j=0}^8$, $\{b_j\}_{j=0}^4$, $\{d_j\}_{j=0}^3$, $\{f_j\}_{j=0}^2$.

III. Parameters identification procedure

The identification procedure for the model parameters is arranged in three main steps starting from the assumption that some parameters of the model are considered to be constant and equal to their nominal values: i) the parameters of the model of the electrical subsystem (4)–(5) are identified by neglecting the temperature dependencies; ii) the parameters of the thermal subsystem model (13) are identified by fixing the electrical parameters to the values identified at the previous step; iii) the decoupling assumption introduced at step i) is verified a posteriori. If the decoupling hypothesis fails, one could try to identify the thermal and electrical parameters within a minimization problem that considers at once all parameters of the process. Clearly the increased complexity of this enlarged problem requires more computational capabilities and may introduce well-posedness issues. In general, the nonlinear optimization procedure could get stuck in local minima; in this case one could restart the identification by using different guess values.

The same procedure has been implemented for the 3RC electrical model (2)–(3) and for the proposed switched model. In the following the steps are detailed for the case of the proposed model only.

The fixed parameters, set at their nominal values, are the battery capacity and the efficiency.

The second step of the procedure consists of some simplifications required for the identification of the parameters of the model (4)–(5). In particular, the dependencies on the temperature of the parameters of this subsystem have been neglected, i.e. $\{a_j\}_{j=3,4,8} = 0$, $b_2 = 0$, $\{d_j\}_{j=2,3} = 0$. Moreover the influence of Soc on the capacitance C_2 has been neglected too, i.e. $\{f_j\}_{j=1,2} = 0$.

The identification procedure consists of a multi-parametric optimization process to find the minimum mismatch between the predicted behavior of the modelled process and the real experimental output. The model of the cell is created in Simulink while the optimization is based on a Matlab nonlinear programming solver "fminsearch". Say P the number of tests used for the identification phase. The vector π_e of the

parameters of the electrical model to be identified is given by

$$\pi_e = \{\{a_j\}_{j=0}^{2}, \{a_j\}_{j=5}^{7}, \{b_j\}_{j=0,1,3,4}, \{d_j\}_{j=0}^{1}, f_0, \hat{R}_2, R_s, C_s, \{Soc_j(0)\}_{j=1}^{P}\}. \quad (14)$$

It should be noticed that the initial values of the Soc for each test are considered as parameters to be identified. Instead the initial conditions of the voltage capacitors are set to zero, i.e. $v_1(0) = 0$ and $v_s(0) = 0$, because each test starts after that the relaxation phase of the previous test has elapsed and the thermal equilibrium has been reached, i.e. $v(0) = OCV(Soc(0), T_a)$ from (5).

The cost function for the minimization is defined as

$$J_e(\pi_e) = \sum_{j=1}^{P} \frac{1}{\tau_j} \int_0^{\tau_j} (v_j(t, \pi_e) - v_j^*(t))^2 \mathrm{d}t \quad (15)$$

where τ_j is the total duration of the j-th test, $j = 1, \ldots, P$ and $v_j^*(t)$, $t \in [0, \tau_j]$ is the experimental measurement of the battery voltage during the j-th test.

Constraints on some model parameters, e.g. electrical resistance, thermal or electric capacitance, can be assigned so that they are restricted to take values in a realistic interval. A barrier function has been added to the cost function (15) in order to take into account such constraints, i.e. the barrier function add an increasing positive error to the cost function when the tentative value of a parameter becomes close to the not permitted region [21].

The parameters obtained by the optimization procedure is given by

$$\pi_e^{\mathrm{opt}} = \arg\min_{\pi_e} J_e(\pi_e). \quad (16)$$

The cost function is computed for a series of P charging cycles and P discharging cycles, any of them including the relaxation phase of the cell. Therefore two different sets of parameters (16) have been obtained for the charging and discharging model, respectively.

The third step of the identification procedure is dedicated to the parameters of the thermal model (13). For this phase the vector of parameters to be identified is given by

$$\pi_{th} = \{C_{th}, R_{th}, \{a_j\}_{j=3,4,8}, b_2\}. \quad (17)$$

The cost function has been chosen as

$$J_{th}(\pi) = \sum_{j=1}^{P} \frac{1}{\tau_j} \int_0^{\tau_j} (T(t, \pi_{th}) - T^*(t))^2 \mathrm{d}t \quad (18)$$

where τ_j is the total duration of the j-th test, $j = 1, \ldots, P$ and $T^*(t)$, $t \in [0, \tau_j]$ is the experimental measurement of the battery temperature during the j-th test.

By using the identified parameters of the thermal model, the fourth step of the identification procedure can be applied, i.e. to verify that the corresponding contributions in (9) are negligible in the sense that the thermal effects can be neglected in evaluating the battery voltage under the specific operating conditions considered.

IV. Experimental results

In this section it is presented the experimental setup realized for implementing the tests whose data are used for the model parameters identification procedure.

A. Experimental setup

The battery cell under test is a SAFT Li-ion battery with reference number MP176065SC-04 which is composed by a single cell with some protection device added by third part assembly. The cell has a nominal voltage of 3.7 V and a capacity (at C/5 rate, $+25$ °C, 2.5 V cut-off) 6.8 Ah corresponding to a nominal energy of 25.16 Wh, the dimensions are $19.6 \text{ mm} \times 60.1 \text{ mm} \times 65.2 \text{ mm}$ and the weight is 150 g.

The experimental setup consists of a programmable source current generator (TTi EX752M), a programmable dummy load (PRODIGIT 3350), a set of temperature sensors attached on the device under test (DUT) and one in the external environment, a bidirectional current and voltage sensors circuits, a three-way power analog switch and, finally, a PC with a data logger software. The programmable dummy load is an active electronic device capable to sink from a voltage source the programmed current (in the range of working condition, independently from the cell's voltage). The temperature of the DUT is obtained by computing the mean of the measures coming from eight temperature sensors positioned on the two sides of the battery cell.

At the end of each charging (discharging) phase the current is set to zero by disconnecting the cell from the circuit. The acquisition of voltage and temperatures continue for a sufficiently long time interval such that the entire relaxation phase is monitored and the corresponding data can be used for the minimization implemented in the parameters identification procedure.

B. Results

Three charging and discharging tests with constant currents equal to ± 0.5 A, ± 1 A and ± 2 A have been carried out.

The battery parameter which has been fixed to its nominal values is $Q = 6.3$ Ah. Some guess values for the parameters vector π_e have been used for starting the minimization procedure of the identification process, see (14). The guess values for $\{a_j\}_{j=0}^{2}$ and $\{a_j\}_{j=5}^{7}$ are obtained by minimizing the error with respect to a nominal characteristics $OCV(Soc, i, T)$ taken from [22] (Figure 3 therein). The guess values for $\{b_0, b_1, b_3, b_4\}$ are obtained by using the nominal curve $R_0(Soc)$ taken from [22] (Figure 5 therein).

The identification procedure provides the values of the parameters of the classical 3RC model shown in Fig. 1 and the proposed switched model shown in Fig. 2, so as reported in Table I. The units of each parameter can be directly deduced from the corresponding equation, see (6)–(9).

The characteristics $OCV(Soc)$ resulting from the identified parameters are shown in Fig. 3. The nonlinear shapes of charging and discharging characteristics of the open circuit voltage show similar behaviors to those presented in [23] (Figure 2 therein).

Symbol	3RC (ch.)	3RC (dis.)	Sw. (ch.)	Sw. (dis.)
a_0	3.589	3.175	3.222	3.188
a_1	-0.049	0.411	0.447	0.413
a_2	-595.335	-34.778	-45.144	-32.906
a_5	0.826	0.533	0.505	0.537
a_6	-0.649	-0.529	-0.559	-0.518
a_7	0.431	0.570	0.550	0.518
b_0	0.447	0.409	0.416	0.486
b_1	-0.093	$3.572 \cdot 10^{-5}$	-0.015	-0.027
b_2	0.016	$-4.061 \cdot 10^{-5}$	0.001	0.001
b_3	-286.229	-43.917	-173.507	-69.588
b_4	-0.327	-0.409	-0.344	-0.402
d_0	0.015	0.041	0.010	0.009
d_1	0.018	0.005	0.000	-0.000
f_0	10.757	2 365.100	52.287	2 807.024
R_1	0.016	0.032	-	-
C_1	0.878	7.163	-	-
R_3	0.001	0.002	-	-
C_3	0.409	0.192	-	-
$\hat{R}_2$	-	-	20.674	92.851
R_s	-	-	0.004	0.002
C_s	-	-	558.572	905.917
$Soc_1(0)$	0.009	0.841	0.023	0.841
$Soc_2(0)$	0.041	0.925	0.033	0.927
$Soc_3(0)$	0.047	0.926	0.045	0.936

TABLE I

IDENTIFIED PARAMETERS FOR THE 3RC MODEL AND THE PROPOSED SWITCHED MODEL FOR CHARGING AND DISCHARGING PHASES.

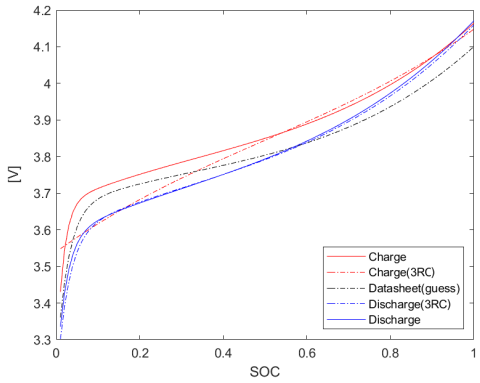

Fig. 3. Characteristics $OCV(Soc)$ corresponding to the different sets of the identified parameters.

The battery voltages obtained with charging and discharging operations under step changes of the battery current having different amplitudes are shown in Figs 4–6. The proposed switched model provides a smaller error and one parameter less to be identified with respect to the classical equivalent circuit model. In all simulations for the identification of the electrical model parameters, the battery temperature is assumed to be constant and equal to the ambient temperature, i.e. $\Delta_T = 0$. The effectiveness of the proposed model is confirmed by a comparison of the values of the cost function (15) obtained for the different experiments is reported in Table II.

The identification of the parameters vector π_{th} corresponding to the thermal model has been obtained by minimizing the cost function (18) corresponding to the tests with different current steps. The parameters of the thermal model (13)

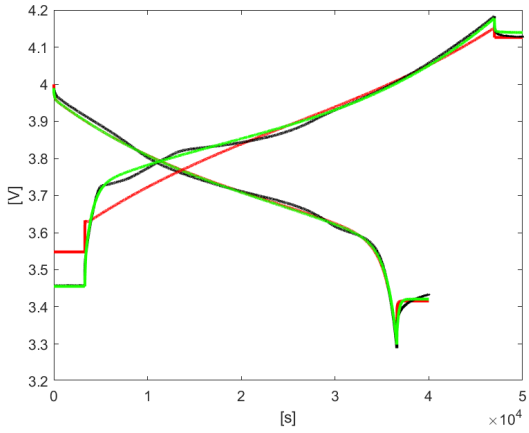

Fig. 4. Battery voltage vs. time for charging and discharging tests with a battery current step equal to ± 0.5 A: experiments (black), 3RC model (red), switched model (green).

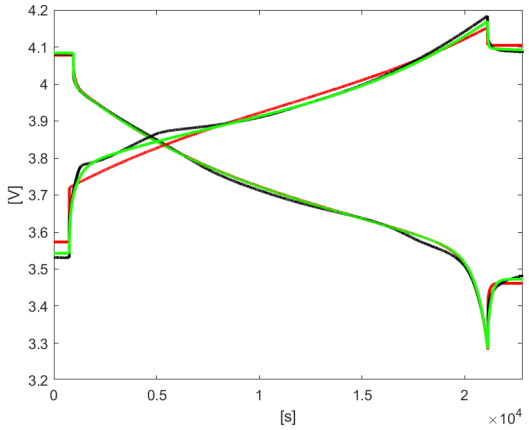

Fig. 5. Battery voltage vs. time for charging and discharging tests with a battery current step equal to ± 1 A: experiments (black), 3RC model (red), switched model (green).

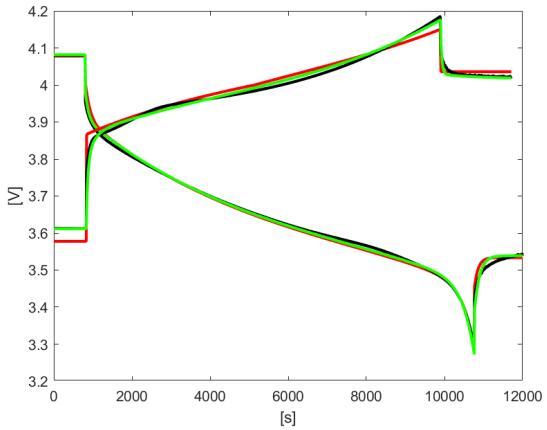

Fig. 6. Battery voltage vs. time for charging and discharging tests with a battery current step equal to ± 2 A: experiments (black), 3RC model (red), switched model (green).

0.5A 3RC	0.5A Sw.	1.0A 3RC	1.0A Sw.	2.0A 3RC	2.0A Sw.
7.0111	0.4823	1.1937	0.2073	0.36910	0.0860
0.3405	0.2912	0.1648	0.1300	0.1275	0.0555

TABLE II

VALUES OF THE COST FUNCTION J_e FOR THE CHARGING (FIRST ROW) AND DISCHARGING (SECOND ROW) EXPERIMENTAL TESTS.

obtained by applying the identification procedure are: $a_3 = -0.162$ W/A, $a_4 = -0.105$ W/K, $a_8 = 0.249$ W/AK, $b_2 = 3.77$ W/A^2, $C_{th} = 46.31$ J/K, $R_{th} = 157.31$ W/K. The temperature measurements obtained from the eight sensors mounted on the cell allows one to say that the temperature distribution over the cell surface can be assumed uniform. Figure 7 shows the results for the test with the current equal to 1 A. The results demonstrate that the model is able to reproduce the battery temperature time evolution with a good accuracy, either for the temperature decrease occurring during the initial phase of the charging process, i.e. the reversible entropic heat phenomenon, and for the successive temperature increase.

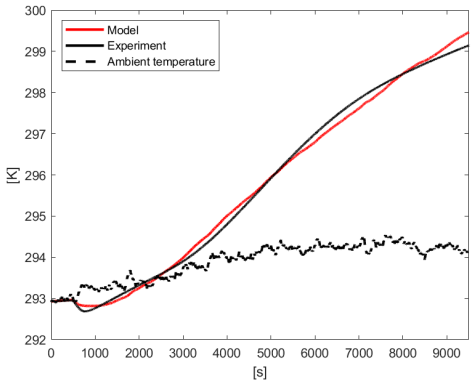

Fig. 7. Temperature time evolution for the charging process at 1 A: ambient temperature (black dashed), experiment (black), thermal model (red).

V. CONCLUSION

A switched electrical model for Li-ion batteries has been proposed. The switch is activated for discriminating the relaxation phase which is usually modeled by using a larger number of equivalent lumped parameters. The proposed model includes the thermal effects too. An identification procedure for the estimation of the model parameters has been proposed. The identified parameters are validated by using charging and discharging experiments. The experimental results have shown the effectiveness of the proposed model and identification procedure.

REFERENCES

[1] T. L. Vincent, P. J. Weddle, and G. Tang, "System theoretic analysis of battery charging optimization," *Journal of Energy Storage,*, vol. 14, pp. 168–178, 2017.

[2] H. E. Perez, X. Hu, S. Dey, and S. J. Moura, "Optimal charging of Li-Ion batteries with coupled electro-thermal-aging dynamics," *IEEE Transactions on Vehicular Technology*, vol. 66, no. 9, pp. 7761–7770, 2017.

[3] A. Berrueta, A. Urtasun, A. Ursúa, and P. Sanchis, "A comprehensive model for Lithium-ion batteries: From the physical principles to an electrical model," *Energy*, vol. 144, pp. 286–300, 2018.

[4] B. Aissa, L. Fethi, and M. Abdelhamid, "Proposal criterion & method to estimate battery SOC in spacecraft application," in *IEEE International Conference on Environment and Electrical Engineering*, Palermo, Italy, 12-15 June 2018, pp. 1–5.

[5] S. Baccari, F. Vasca, E. Mostacciuolo, L. Iannelli, S. Sagnelli, R. Luisi, and V. Stanzione, "A characterization system for LEO satellites batteries," in *European Space Power Conference*, Juan-Les-Pins, France, 1-4 Oct. 2019, pp. 1–6.

[6] D. Dvorak, T. Bäuml, A. Holzinger, and H. Popp, "A comprehensive algorithm for estimating lithium-ion battery parameters from measurements," *IEEE Transactions on Sustainable Energy*, vol. 9, no. 2, pp. 771–779, 2018.

[7] L. Gao, S. Liu, and R. A. Dougal, "Dynamic lithium-ion battery model for system simulation," *IEEE Transactions on Components and Packaging Technologies*, vol. 25, no. 3, pp. 495–505, 2002.

[8] G. Plett, *Battery Management Systems, Volume II: Equivalent-Circuit Methods*. Artech House: London, 2015.

[9] M. Murnane and A. Ghazel, "A closer look at state of charge (SOC) and state of health (SOH) estimation techniques for batteries," *Analog Devices*, 2017.

[10] E. Mostacciuolo, F. Vasca, S. Baccari, L. Iannelli, S. Sagnelli, R. Luisi, and V. Stanzione, "Fault analysis to improve reliability of a LEO satellite EPS," *IFAC-PapersOnLine*, vol. 52, no. 12, pp. 200–205, Aug 2019.

[11] H. M. Usman, S. Mukhopadhyay, and H. Rehman, "Universal adaptive stabilizer based optimization for li-ion battery model parameters estimation: An experimental study," *IEEE Access*, vol. 6, pp. 49 546–49 562, 2018.

[12] L. Xiubin, L. Yue, W. Nantian, Z. Qingqi, and L. Tingpeng, "The diffusion polarization model of lithium-ion battery relaxation effect," in *12th IEEE International Conference on Electronic Measurement Instruments*, Qingdao, China, 16-18 July 2015, pp. 131–135.

[13] H. Rahimi-Eichi, F. Baronti, and M. Y. Chow, "Modeling and online parameter identification of Li-Polymer battery cells for SOC estimation," in *IEEE International Symposium on Industrial Electronics*, Hangzhou, China, 28-31 May 2012, pp. 1336–1341.

[14] E. Mostacciuolo, F. Vasca, S. Baccari, L. Iannelli, S. Sagnelli, R. Luisi, and V. Stanzione, "An optimization strategy for battery charging in small satellites," in *European Space Power Conference*, Juan-Les-Pins, France, 1-4 Oct. 2019, pp. 1–8.

[15] F. Feng, R. Lu, and C. Zhu, "A combined state of charge estimation method for lithium-ion batteries used in a wide ambient temperature range," *Energies*, vol. 7, no. 5, pp. 3004–3032, 2014.

[16] A. Zurfi and J. Zhang, "Experimental identification and validation of a battery model for a battery-buffered frequency-controlled smart load," in *IEEE 7th International Symposium on Power Electronics for Distributed Generation Systems*, Vancouver, Canada, 27-30 June 2016, pp. 1–7.

[17] A. Farmann and D. U. Sauer, "A study on the dependency of the open-circuit voltage on temperature and actual aging state of lithium-ion batteries," *Journal of Power Sources,*, vol. 347, pp. 1–13, 2017.

[18] M. Chen and G. A. Rincon-Mora, "Accurate electrical battery model capable of predicting runtime and I-V performance," *IEEE Transactions on Energy Conversion*, vol. 21, no. 2, pp. 504–511, 2006.

[19] M. Ceraolo, "New dynamical models of lead-acid batteries," *IEEE Transactions on Power Systems*, vol. 15, no. 4, pp. 1184–1190, 2000.

[20] G. Liu, M. Ouyang, L. Lu, J. Li, and X. Han, "Analysis of the heat generation of lithium-ion battery during charging and discharging considering different influencing factors," *Journal of Thermal Analysis and Calorimetry*, vol. 116, pp. 1001–1010, 2014.

[21] S. Baccari, L. Iannelli, and F. Vasca, "A parallel algorithm for implicit model predictive control with barrier function," in *IEEE International Conference on Control Applications*, Dubrovnik, Croatia, 3-5 Oct. 2012, pp. 1405–1410.

[22] A. Vanessa, C. Jacky, J. Hyvert, G. Aurelie, P. J. Paul, R. Stephane, and B. Yannick, "MP XLR battery range for constellation," in *European Space Power Conference*, Juan-Les-Pins, France, 1-4 Oct. 2019, pp. 1–8.

[23] A. Li, S. Pelissier, P. Venet, and P. Gyan, "Fast characterization method for modeling battery relaxation voltage," *Batteries*, vol. 2, no. 7, pp. 1–15, 2016.